

E1-2008-61

THE RATIO R_{dp} OF THE QUASI-ELASTIC $nd \rightarrow p(nn)$
TO THE ELASTIC $np \rightarrow pn$ CHARGE-EXCHANGE
PROCESS YIELDS AT 0° OVER 0.55–2.0 GeV
NEUTRON BEAM ENERGY REGION:
1. EXPERIMENTAL RESULTS

Submitted to «Yadernaya Fizika»

Шаров В. И. и др.

E1-2008-61

Отношение R_{dp} выходов процессов квазиупругой $nd \rightarrow p(nn)$ и упругой $np \rightarrow pn$ перезарядки под углом 0° в области энергий пучка нейтронов 0,55–2,0 ГэВ.

1. Экспериментальные результаты

Представлены новые экспериментальные результаты по отношению R_{dp} выхода $nd \rightarrow p(nn)$ реакции квазиупругой перезарядки под углом 0° к выходу упругой $np \rightarrow pn$ перезарядки. Измерения проводились на нуклотроне ЛВЭ ОИЯИ при значениях кинетической энергии пучка нейтронов 0,55, 0,8, 1,0, 1,2, 1,4, 1,8 и 2,0 ГэВ. Данные накапливались с помощью магнитного спектрометра установки «Дельта–Сигма» с двумя наборами многопроволочных пропорциональных камер, расположенных до и после анализирующего магнита. Неупругие процессы значительно подавлялись посредством дополнительных детекторов, окружающих водородную и дейтериевую мишени. Времяпролетная система применялась для идентификации детектируемых частиц. Обсуждаются обработка накопленной статистики и анализ возможных систематических ошибок. Полученные значения R_{dp} остаются почти постоянными во всем диапазоне измерений. Новые результаты сравниваются с существующими данными, измеренными при энергиях ниже 1,0 ГэВ. Сравнение этих данных с расчетными значениями R_{dp} , полученными с использованием наборов инвариантных NN амплитуд из решений GW/VPI фазового анализа, выполнено в отдельной статье.

Работа выполнена в Лаборатории высоких энергий им. В. И. Векслера и А. М. Балдина ОИЯИ.

Препринт Объединенного института ядерных исследований. Дубна, 2008

Sharov V. I. et al.

E1-2008-61

The Ratio R_{dp} of the Quasi-Elastic $nd \rightarrow p(nn)$ to the Elastic $np \rightarrow pn$ Charge-Exchange Process Yields at 0° over 0.55–2.0 GeV Neutron Beam Energy Region:

1. Experimental Results

New experimental results on ratio R_{dp} of the quasi-elastic charge-exchange yield at 0°_{Lab} for the $nd \rightarrow p + (nn)$ reaction to the elastic $np \rightarrow pn$ charge-exchange yield are presented. The measurements were carried out at the Nuclotron of JINR VBLHE at neutron beam kinetic energies of 0.55, 0.8, 1.0, 1.2, 1.4, 1.8 and 2.0 GeV. The data were accumulated by means of the «Delta–Sigma» set-up magnetic spectrometer with two sets of multiwire proportional chambers located upstream and downstream of the analyzing magnet. Inelastic processes were considerably reduced by means of the additional detectors surrounding the hydrogen and deuterium targets. The time-of-flight system was applied to identify a detected particle. The accumulated data treatment and analysis of possible systematic errors are discussed. The obtained R_{dp} values remain nearly constant with the energy. The new data are compared with the existing ones, which were measured up to 1 GeV. The comparison of these data with the calculations of R_{dp} obtained by using the invariant amplitude sets from the GW/VPI phase-shift analysis was made in a separate paper.

The investigation has been performed at the Veksler and Baldin Laboratory of High Energies, JINR.

Preprint of the Joint Institute for Nuclear Research. Dubna, 2008

V. I. Sharov^{1,*}, A. A. Morozov¹, R. A. Shindin¹, V. G. Antonenko², S. B. Borzakov¹,
Yu. T. Borzunov¹, E. V. Chernykh¹, V. F. Chumakov¹, S. A. Dolgii¹, M. Finger^{1,3},
M. Finger, Jr.¹, L. B. Golovanov¹, D. K. Guriev¹, A. Janata¹, A. D. Kirillov¹,
A. D. Kovalenko¹, V. A. Krasnov¹, N. A. Kuzmin¹, A. K. Kurilkin¹, P. K. Kurilkin¹,
A. N. Livanov¹, V. M. Lutsenko¹, P. K. Maniakov¹, E. A. Matyushevsky¹,
G. P. Nikolaevsky¹, A. A. Nomofilov¹, Tz. Pantelev^{1,4}, S. M. Piyadin¹, I. L. Pisarev¹,
Yu. P. Polunin^{2,†}, A. N. Prokofiev⁵, V. Yu. Prytkov¹, P. A. Rukoyatkin¹, M. Slunečka^{1,3},
V. Slunečková¹, A. Yu. Starikov¹, L. N. Strunov¹, T. A. Vasiliev¹, E. I. Vorobiev¹,
I. P. Yudin¹, I. V. Zaitsev¹, A. A. Zhdanov⁵, V. N. Zhmyrov¹

¹Joint Institute for Nuclear Research, Dubna

²Russian Scientific Center «Kurchatov Institute», Moscow

³Charles University, Faculty of Mathematics and Physics, Prague, Czech Republic

⁴Institute for Nuclear Research and Nuclear Energy, Bulgarian Academy of Sciences,
Sofia, Bulgaria

⁵St. Petersburg Nuclear Physics Institute, Gatchina, Russia

*E-mail: sharov@sunhe.jinr.ru

†Deceased

INTRODUCTION

The paper presents new experimental results on the ratio R_{dp} of the charge-exchange (CEX) quasi-elastic differential cross section for the reaction $nd \rightarrow p + (nn)$ at 0_{Lab}° to the elastic CEX differential cross section $np \rightarrow pn$. The intense quasi-monochromatic neutron beam was produced by break-up of the deuterons accelerated by the Nuclotron of the Veksler and Baldin Laboratory of High Energies (VBLHE) at the Joint Institute for Nuclear Research (JINR) in Dubna. In both reactions mentioned above the outgoing protons with the momenta \mathbf{p}_p near to the neutron beam momentum $\mathbf{p}_{n,\text{beam}}$ were detected in the directions close to the direction of incident neutrons, i.e., in the vicinity of the scattering angle $\theta_{p,\text{Lab}} = 0^{\circ}$. Thus, we consider such an outgoing proton as the former beam neutron which was scattered at $\theta_{p,\text{CM}} = 0^{\circ}$ and got the electric charge in the charge-exchange process.

Having taken into account the detector efficiencies and other well known instrumental effects the yields of the quasi-elastic and elastic scattering measured with the H_2 and D_2 targets, were corrected. The above yields were taken over the spectrometer angular acceptance $0 < \varphi \leq 2\pi$ and $0 < \theta \leq 30$ mrad. These corrected yields are proportional to the corresponding differential cross sections. The measurements were carried out at the neutron beam kinetic energies of 0.55, 0.8, 1.0, 1.2, 1.4, 1.8 and 2.0 GeV.

The measurements were performed within the programme of the JINR project «Delta-Sigma experiment» [1–3] (see also Ref. [30] in arXiv:0706.2195 [nucl-th]). The aim of this experimental programme is to determine the imaginary and real parts of the $np \rightarrow np$ forward ($\theta_{n,\text{CM}} = 0$) and backward ($\theta_{n,\text{CM}} = \pi$) all elastic scattering amplitudes over the 1.2–3.7 GeV energy region. In this highest energy interval of free polarized neutron beams the measurements are possible at the Nuclotron only.

At the forward and backward angles only three complex amplitudes are independent. The scattering amplitudes in the forward and backward hemispheres are determined by the angular symmetry conditions: they differ for isospins $I = 1$ and $I = 0$. We assume that the $I = 1$ amplitudes are known. Consequently, for the direct reconstruction of the np amplitudes, altogether, at least, six independent observables at either the forward or backward directions, are needed. Two

np observables are well known, one of them is the spin independent np total cross section $\sigma_{0\text{tot}}$, the second one is the $np \rightarrow np$ differential cross section at $\theta_{n,\text{CM}} = \pi$.

The research programme «Delta-Sigma» foresees the measurements of total cross section differences $\Delta\sigma_{L,T}(np)$ and spin correlation parameters $A_{00kk}(np \rightarrow np)$ and $A_{00nn}(np \rightarrow np)$ at $\theta_{n,\text{CM}} = \pi$ for the longitudinal (L) and transverse (T) beam and target polarization directions, respectively. The $\Delta\sigma_{L,T}(np)$ observables together with $\sigma_{0\text{tot}}$ are linearly related to the imaginary part of the independent forward scattering amplitudes via optical theorems. These three observables unambiguously determine the imaginary parts of all the amplitudes.

The $\Delta\sigma_{L,T}(np)$ observables are to be measured in transmission experiments. Measurements of the $-\Delta\sigma_L(np)$ energy dependence were carried out at ten different values of energy [4–9]. The L -polarized neutron beam from the Synchrophasotron of the JINR VBLHE and the Dubna L -polarized proton target were used. New measurements of the $\Delta\sigma_{L,T}(np)$ are expected after the new high intensity source of polarized deuterons is operational at the Nuclotron. This device will be based on the CIPIOS [10] equipment imported to Dubna from the Indiana University Cyclotron Facility.

The $A_{00kk}(np \rightarrow np)$ and $A_{00nn}(np \rightarrow np)$ values are to be defined in the backward direction. These observables could be measured simultaneously with the corresponding $\Delta\sigma_{L,T}(np \rightarrow np)$ experiments. Using the imaginary parts of the forward amplitudes transformed into the backward direction, the np differential cross section and the two spin correlations at $\theta_{\text{CM}} = \pi$ are sufficient to obtain the three real parts of the amplitudes. In contrast to the optical theorems at $\theta = 0^\circ$, the scattering amplitudes in the backward direction are related to the scattering observables by bilinear equations. Each of them may have, in principle, an independent ambiguity in the sign. The total ambiguity is then eight-fold at most and any independent experiment decreases it by the factor of two.

To reduce the total ambiguity in the scattering amplitude determination, the «Delta-Sigma» collaboration performed the measurements of the ratio $R_{dp} = (d\sigma/d\Omega)(nd)/(d\sigma/d\Omega)(np)$ for the charge-exchange processes on the deuterium and hydrogen targets. A high intensity unpolarized neutron beam was scattered either in the liquid D_2 and H_2 or solid CD_2 and CH_2 targets. The knowledge of R_{dp} value could provide one additional constraint and reduce the ambiguity discussed above. Moreover, the described experiment is a powerful test for the future spin correlation measurements. The results of the experiments under discussion are listed below.

Sections 1 and 2 describe the measuring method and the essential details on the beam and experimental set-up. Section 3 is devoted to the data acquisition, treatment and analyses. The obtained R_{dp} results are given in Sec. 4, conclusions are enumerated in Sec. 5.

1. METHOD OF MEASUREMENTS

As mentioned above, the observable R_{dp} is the ratio of the quasi-elastic $\theta_{p,\text{CM}} nd \rightarrow p + nn$ (labeled by nd) charge-exchange differential cross section to the free $np \rightarrow pn$ (labeled by np) elastic one. That is as follows:

$$R_{dp}(\theta_p) = \frac{(d\sigma/d\Omega)(nd \rightarrow pnn)}{(d\sigma/d\Omega)(np \rightarrow pn)}. \quad (1.1)$$

In both $nd \rightarrow p + nn$ and $np \rightarrow pn$ reactions the outgoing (scattered) protons with momenta \mathbf{p}_p near to the neutron beam momentum $\mathbf{p}_{n,\text{beam}}$ are detected in the directions close to the direction of incident neutrons, i.e., in the vicinity of the scattering angle $\theta_{p,\text{Lab}} = 0^\circ$. Thus, we consider such an outgoing proton as the former beam neutron which was scattered at $\theta_{p,\text{CM}} = 0^\circ$ and got the electric charge in the charge-exchange process.

The outgoing protons are detected to measure the $np \rightarrow pn$ yield at $\theta_{p,\text{Lab}} = 0$. With the hydrogen target, for example, the number of protons N , detected over the solid angle $\Delta\Omega$, subtended by the spectrometer detectors, and normalized to flux M of incident neutrons, is given by the following equation:

$$\frac{N}{M} = \Delta\Omega \cdot \epsilon \cdot n_{\text{H}} \cdot \frac{d\sigma}{d\Omega}, \quad (1.2)$$

where n_{H} is the number of hydrogen nuclei in the target, ϵ is the proton detection efficiency and $d\sigma/d\Omega$ is the differential cross section of the investigated process. The measured differential cross section is as follows:

$$\frac{d\sigma}{d\Omega}(\Delta\Omega) = \frac{N}{M} \cdot \frac{1}{\Delta\Omega \cdot \epsilon \cdot n_{\text{H}}}. \quad (1.3)$$

The solid angle element $\Delta\Omega = \sin(\theta) \cdot \Delta\theta \cdot \Delta\phi$, where θ and ϕ are polar and azimuthal angles of the scattered protons. The extrapolation of $d\sigma/d\Omega(\Delta\Omega)$ towards $\Delta\Omega = 0$ ($\theta_p = 0$) gives the desired experimental value of $d\sigma/d\Omega(\theta = 0)$.

In this experiment the measurements of the yields of $np \rightarrow pn$ and $nd \rightarrow pnn$ processes at small $\theta_{p,\text{Lab}}$ were carried out during the same data taking run, using either the cryogenic liquid hydrogen H_2 , deuterium D_2 and empty (E) targets or the polyethylene CH_2 , deuterated polyethylene CD_2 and carbon C targets. The measured $R_{dp}(\theta_p)$ values are determined by

$$R_{dp}(\theta_p) = \frac{(N_{\text{D}} - k_{\text{D}} \cdot N_{\text{E}}) \cdot M_{\text{H}} \cdot \epsilon_{\text{H}} \cdot n_{\text{H}}}{(N_{\text{H}} - k_{\text{H}} \cdot N_{\text{E}}) \cdot M_{\text{D}} \cdot \epsilon_{\text{D}} \cdot n_{\text{D}}}, \quad (1.4)$$

where N_{H} , N_{D} , N_{E} , and M_{H} , M_{D} , M_{E} , and ϵ_{H} , ϵ_{D} , ϵ_{E} are the yields, monitor rates and detector efficiencies for the H_2 , D_2 , and E or CH_2 , CD_2 , and C

targets, respectively. n_{H} and n_{D} are the numbers of hydrogen and deuterium nuclei in the H_2 and D_2 or CH_2 and CD_2 targets, k_{H} and k_{D} are the factors depending on the ratio of the monitor counts and detector efficiencies for the filled H_2 or D_2 (CH_2 or CD_2) to the empty $E(C)$ targets.

The solid angle element $\Delta\Omega$ is the same for the H_2 , D_2 and E targets and cancelled from the numerator and denominator in Eq. (1.4). It is important that the M_{H} and M_{D} absolute values are not required to determine R_{dp} and only the relative values are sufficient. Just for this reason the measurements using neutron beams have a considerable advantage with respect to the experiments with the incident proton or deuteron beams.

For the measurements it is also important to maintain stable experimental conditions: (e.g., detector geometry and regimes, neutron beam and targets characteristics). It is equally important to provide the change of the targets as fast as possible to reduce existing influence of temporary drifts of detector efficiencies.

2. EXPERIMENTAL SET-UP

A magnetic spectrometer to detect protons from $np \rightarrow pn$ elastic and $nd \rightarrow pnn$ quasi-elastic charge-exchange processes at $\theta_{\text{Lab}} = 0$, was installed and tested at the intense free neutron beam line of the JINR VBLHE Nuclotron facility. The spectrometer is a part of the «Delta-Sigma» set-up (see Fig. 1) to measure the np spin-dependent total cross section differences. The «Delta-Sigma» experimental set-up was described in detail in our previous publications [4–9].

Figure 1 shows the both extracted deuteron and free neutron beam lines [11], the beryllium target (BT) for the neutron production, the collimators $C1$ – $C4$, the polarized proton target PPT , the monitors $M1$, $M2$ of neutron beam intensity, transmission detectors $T1$, $T2$, $T3$ and the detectors for neutron beam profile monitoring NP .

The accelerated deuterons were extracted at the beam momenta p_d of 2.31, 2.93, 3.39, 3.84, 4.29, 5.15 and 5.57 GeV/ c , which were known with sufficient accuracy of $\approx \pm 1\%$. The average intensity of the primary deuteron beam was $\approx 2 \times 10^{10}$ d/cycle. It was continuously monitored by two calibrated ionization chambers placed in the two focal points upstream of the neutron production target BT .

The beam of free quasi-monochromatic neutrons was obtained by break-up at 0° of deuterons in BT . The set of collimators $C1$ – $C4$ determined the necessary profile size of the neutron beam. The dimension of the inner hole of the last brass collimator was 26 mm in diameter. The primary deuterons passing through the BT without interaction as well as the charged secondaries from inelastic reactions were deflected from the neutron beam direction by the sweeping magnet SM and were directed to the beam dump.

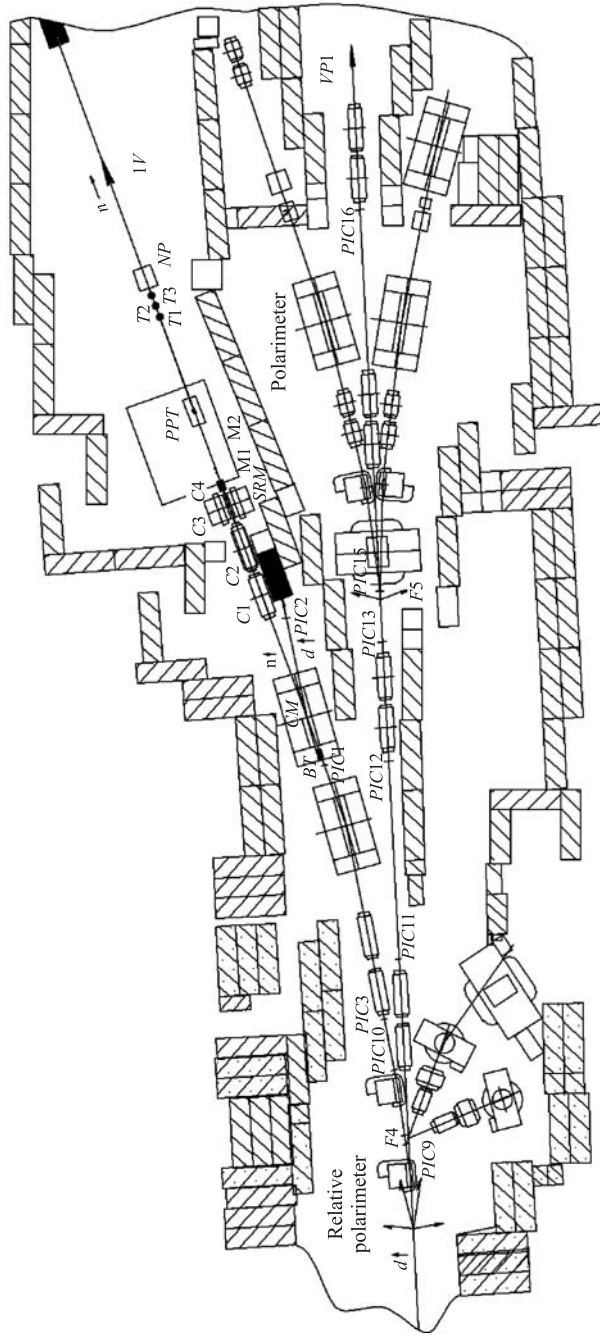


Fig. 1. Experimental set-up for the $\Delta\sigma_L(np)$ measurement. Layout of the set-up in the Experimental Hall. $VP1$ — beam line of extracted vector polarized deuterons with $\mathbf{p}_B(d)$ oriented along the vertical direction $d(t)$; $1V$ — beam line to generate and form the polarized neutron beam, $n(\uparrow)$ — neutrons polarized vertically, $n(\rightarrow)$ — neutrons polarized longitudinally; $F4, F5$ — focuses of the extracted deuteron beam line; BT — beryllium target for neutron production; IC — ionization chamber for the deuteron beam intensity monitoring; $PIC1 - 3, 9 - 16$ — multiwire proportional/ionization chambers to measure the deuteron beam profiles; SM — sweeping magnet; $C1 - C4$ — set of neutron beam collimators; SRM — neutron spin rotating dipole; PPT — polarized proton target; and NP — neutron beam profilometer

Neglecting the BT thickness, neutrons have a laboratory momentum $p_n = p_d/2$ with a gaussian momentum spread of $\text{FWHM} \simeq 5\%$ [12]. This corresponds to the neutron beam energies $T_{\text{kin}}(n)$ of 0.55, 0.8, 1.0, 1.2, 1.4, 1.8 and 2.0 GeV, respectively. BT contained beryllium, 20 cm long with the cross section of 8×8 cm. The energy losses of deuterons during their passage through air, foils in the vacuum tubes of the beam transport line and the BT substance, resulted in decrease of the deuteron beam energy by 20 MeV in the BT center as well as in the mean neutron energy decrease by 10 MeV [4, 7]. But Table 7 below shows the R_{dp} results at the extracted beam energies without taking these losses into account.

The neutron beam intensity was monitored by the two neutron beam monitors $M1, M2$. Each of the detectors $M1, M2$ is independent of another. The monitor units were of the same design and the electronic systems were identical as described in [4–9]. Each unit consisted of a CH_2 converter 60 mm thick placed behind a large veto scintillation counter A . The emitted forward charged particles generated by neutron interactions in the converter substance were detected by two counters $S1$ and $S2$ on coincidence. The converters and $S1, S2$ counters for monitors $M1$ and $M2$ were 30 mm in diameter.

During the data taking runs the intensity of the neutron beam varied from 8×10^5 n/cycle at $T_n = 0.8$ GeV up to 4×10^6 n/cycle at $T_n = 2.0$ GeV.

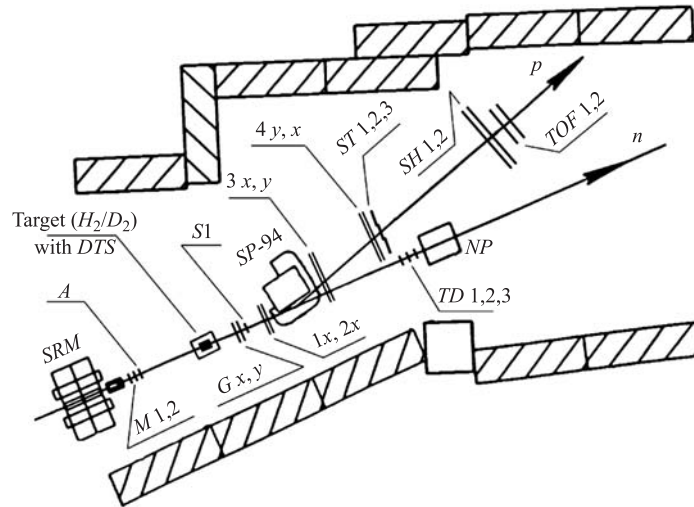


Fig. 2. Magnetic spectrometer for detection of protons from $np \rightarrow pn$ elastic charge exchange at 0° (Lab.). $SP-94$ — analyzing dipole; $Gx, y, 1x, 2x, 3x, y, 4x, y$ — two sets of multiwire proportional chambers; $MPT, H_2/D_2$ — the polarized proton or liquid H_2 or D_2 targets; $S1, TOF1, 2$ and $A, S1, ST$ — time-of flight and trigger counters

The spectrometer (see Fig. 2) consists of one analyzing dipole $SP - 94$; a set of multiwire proportional chambers PCs : $Gx, Gy, 1x, 2x$ placed before the dipole and another set of PCs : $3x, 3y, 4x, 4y$ — after it — for momentum analysis of detected secondaries; trigger counters $A, S1, ST$; time-of-flight system ($S1, TOF1, 2$) for particle identification; liquid H_2 or D_2 targets inserted in the neutron beam line (instead of the proton polarized target used for the $\Delta\sigma$ experiment). The target in use was surrounded by device DTS (detectors for target surrounding) to detect the charged recoil particles and gammas.

The scintillation counters and PCs dimensions are listed in Tables 1, 2. The multiwire proportional chambers have the wire spacing of 2 mm for all PCs . An example of the PCs efficiencies at $T_n = 1.4$ GeV with the CH_2 target is given in Table 3. The accuracies of measurements of angular values and momentum are listed in Table 4.

Table 1. The scintillation counters dimensions

Counter name	Dimensions	z coordinate*, mm	Used in
A	$150 \times 150 \times 6$ mm	-128	«Veto» in trigger
$S1$	100 mm in diameter, 6 mm thickness	1369	Trigger
$S2$	3 units $150 \times 150 \times 6$ mm, total width 420 mm	5500	Trigger
$TOF1$	$500 \times 200 \times 20$	12293	TOF
Time-of-flight base from $S1$ up to $TOF1 = 10925$ mm			
*Along the neutron beam direction starting from the target center			

Table 2. Dimensions and positions of the PCs

PCs name	Number of wires	Working area, mm	z coordinate*, mm	Position
Gx	64	128	1060	Upstream of analysing magnet
Gy	64	128	1232	
$1x$	96	192	1969	
$2x$	96	192	2069	
$3x$	192	384	4378	Downstream of analysing magnet
$4x$	192	384	5200	
$3y$	144	288	4402	
Total: 848				
*Along the neutron beam direction starting from the target center				

Table 3. Efficiencies of the PC's at $T_n = 1.4$ GeV with CH_2 target

NN	PC's name	«On-line»				«Off-line»
		Zero*	All*	One*	Cl2*	(One+Cl2)**
1	1x	0.026	0.974	0.880	0.049	0.948 +/- 0.003
2	2x	0.032	0.968	0.859	0.069	0.951 +/- 0.003
3	3x	0.049	0.951	0.512	0.388	0.948 +/- 0.003
4	3y	0.031	0.969	0.868	0.060	0.972 +/- 0.004
5	gy	0.015	0.985	0.885	0.058	0.957 +/- 0.003
6	gx	0.010	0.990	0.868	0.077	0.959 +/- 0.003
7	4x	0.058	0.942	0.561	0.330	0.917 +/- 0.003
Total:			0.798	0.145		0.887 +/- 0.006
*Zero — there is no signal from any wire in the PC; All — there are signals from some wires; One — there is a signal from only one wire; Cl2 — there are signals from only two neighbouring wires. **During the data treatment, the information from PC 1x «or» 2x and PC 3x «or»/«and» PC 4x was used.						

Table 4. The accuracies of the angular values and momentum measurements

For angular values:			
Measured value	Bin, mrad	Instrumental error, mrad	Information taken from PC's
θ_x	1.97	0.83	Gx AND 1x
θ_x	1.79	0.76	Gx AND 2x
θ_y	0.61	0.26	Gy AND 3y
At momentum measurement of the extracted deuteron beam:			
$\sigma P/P$	Information taken from PC's		
1.40%	Gx AND (1x OR 2x) AND ((3x AND 4x) OR 3x OR 4x)		
1.37%	Gx AND 2x AND 3x AND 4x		

The liquid hydrogen H_2 (or deuterium D_2) as the cryogenic target was enclosed into a thin-wall mylar container 340 mm long and 70 mm in diameter, cooled by liquid helium. The target device had two identical containers for the target substance. One of the containers was filled with the target substance (H_2 or D_2) and the second one was empty. The target device could be moved together with the filled and empty targets across the neutron beam direction to put one of them into the beam. During the data taking runs, the filled and empty targets were interchanged after 3–4 h. The change of the target substance (H_2 or D_2) was made after 1.5–2 d of measurements.

Table 5. The dimensions of the solid and cryogenic targets and the total number of target atoms in the neutron beam path

Cryogenic targets					
Target substance	Length, mm	Diameter, mm	Number of atoms $\times 10^{23} \text{ cm}^{-2}$		
H_2	340	70	14.496		
D_2	340	70	16.892		
Solid targets					
Target substance	Length, mm	Width, mm	Height, mm	Number of atoms $\times 10^{23} \text{ cm}^{-2}$	
CH_2	150	50	40	H : 12.495	C : 6.348
CD	150	50	40	D : 12.490	C : 6.245
C	75	50	40	C : 6.342	

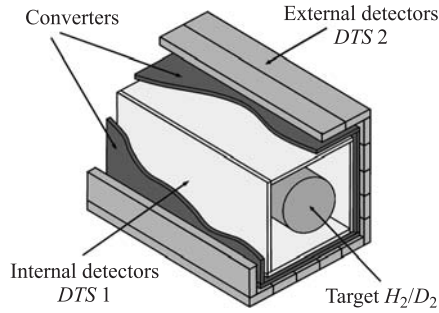


Fig. 3. Two arrays of Detectors for the Target Surrounding *DTS*

At the neutron beam energies of 0.55, 0.8 and 1.4 GeV the data taking was carried out with the polyethylene CH_2 , deuterated polyethylene CD_2 and carbon C targets. These targets could be changed very quickly and frequently after 1–1.5 h. These operations minimized the possible temporary drifts of detector efficiencies and decreased their contributions to the ΔR_{dp} uncertainty. On the other hand, the polyethylene targets gave a considerable number of background inelastic events from the carbon nuclei. The dimensions of the solid and cryogenic targets and the total number of the target atoms on the neutron beam path are listed in Table 5.

The construction of *DTS* (see Fig. 3) contained the internal set of four scintillators ($450 \times 160 \times 10$ mm) to detect the charge recoils, the set of lead converters for gamma interactions and the external set of 20 scintillators ($430 \times 50 \times 20$ mm) to detect the converted electrons. The expected efficiency of

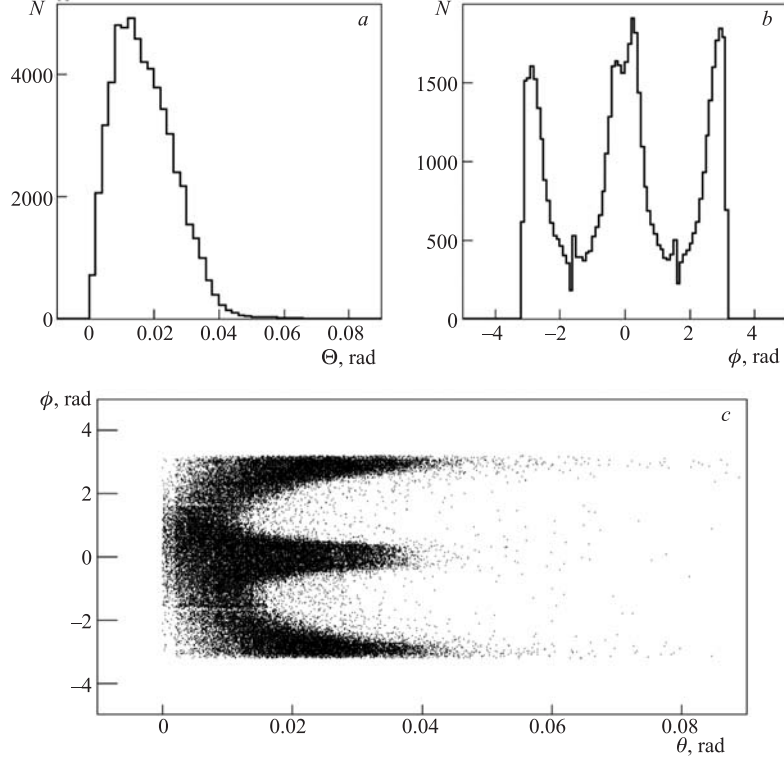


Fig. 4. The spectrometer angular acceptance. The detected events distribution in the θ vs φ plane

this device to detect the inelastic np interactions was estimated to be about 80%.

Some characteristics of the magnetic spectrometer and investigated process are shown in Figs. 4–7. The angular acceptance of the spectrometer in the polar θ and azimuthal φ angular planes is shown in Fig. 4. For the azimuthal range from $\varphi = 0$ to $\varphi = 2\pi$ the polar angular range reduces to the θ values of 10–12 mrad. For the smaller φ regions the polar angle range increases up to 30–35 mrad.

Figure 5 illustrates the momentum spectra of charged secondaries detected by the spectrometer on the H_2 (a) and D_2 (b) liquid targets at the neutron beam energy of 1.2 GeV. The detected particle identification from both the magnetic analysis and the TOF spectra is demonstrated in Fig. 6.

Information from the detectors for the target surrounding DTS helped us to suppress the contributions from the other (inelastic) np -reaction channels. The solid lines in Fig. 7 show the momentum spectra of the charged secondaries obtained without the information from the DTS . The painted areas in the figure

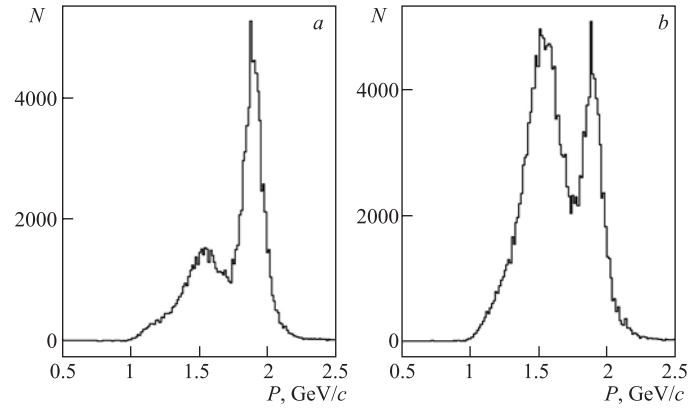


Fig. 5. The momentum spectra of charged secondaries, detected by the spectrometer using H_2 (a) and D_2 (b) liquid targets, at the neutron beam energies of 1.2 GeV

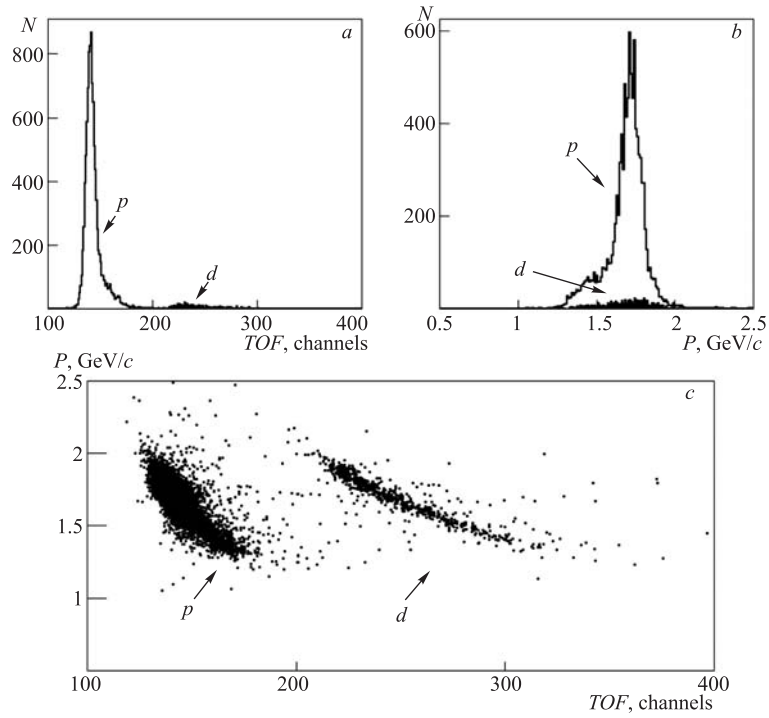


Fig. 6. The detected particle identification at $T_n = 1.0$ GeV using both the magnetic analysis and time-of-flight spectra

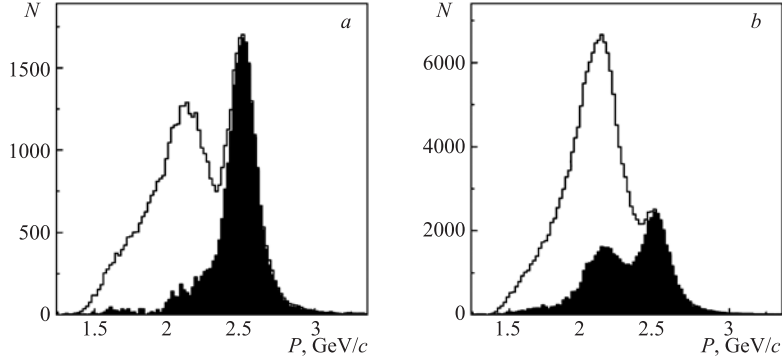


Fig. 7. Suppression of the contributions from the inelastic np -reaction channels using information from the detectors for the target surrounding DTS . The examples of momentum spectra obtained at $T_n = 1.8$ GeV for the liquid hydrogen a and deuterium b targets. The solid lines show the momentum spectra of charged secondaries obtained without using the information from the DTS . The filled areas show the momentum spectra, when the signal from DTS is in anticoincidence with the spectrometer trigger

show the momentum spectra when the signal from DTS is in anticoincidence with the spectrometer trigger. These examples of the spectra were received at $T_n = 1.8$ GeV for the liquid hydrogen (a) and deuterium (b) targets.

3. DATA ACQUISITION, TREATMENT AND ANALYSIS

The data acquisition system is based on CAMAC parallel branch highway controlled by IBM PC with the branch driver [13], completed by E. V. Chernykh, one of the co-authors. The flexible program equipment for the on-line recording and treatment of the accumulated statistics was used. The on-line program in Pascal works under DOS.

The desired statistics was mainly accumulated under the condition $Tr1 = Gx * S1 * ST * \bar{A}$. From time to time the second regime $Tr2 = Gy * S1 * ST * \bar{A} * TOF1$ was used to check the current efficiency of the trigger PC Gx and characteristics of the TOF -system. In the trigger notation the symbol $*$ means the logic AND, the symbols $S1$, ST , TOF mean the logic signals from the indicated scintillation counters, the notation \bar{A} means «NOT A» and the symbols Gx , Gy correspond to the logic OR for all the wires of the indicated PC s.

The main trigger condition $Tr1$ provided good enough efficiency for the investigated process detection. Dimensions of the scintillation counter ST , placed downstream of the analysing magnet, define the angular and momentum acceptances of the spectrometer. To reduce the number of background events in the

$S1$ substance, the $PC\ Gx$ signal was introduced into the condition $Tr1$ and the trigger counter $S1$ was placed downstream of the $PCs\ Gx$ and Gy . The signal from the «*veto*» counter A was introduced in anticoincidence to reduce the charged particle background induced in the substance of the channel and detector elements before the target.

For each trigger signal the PCs coordinate information together with the information from DTS and TOF (TDC, ADC) was registered and accumulated by the data acquisition system. The monitor counts $M1$ and $M2$, the counts from the ionization chambers for primary deuteron beam monitoring and other important counting rates were accumulated in the scalers within the beam extraction cycle and recorded by the «*end of the cycle*» signal.

The statistics was accumulated by the subruns of 0.5–1 h. During data taking for each subrun the current processing of the accumulated statistics was performed by the on-line program during the interval between the accelerator cycles. The program carried out the recording, accumulation, preliminary treatment and convenient on-line displaying of the accumulated experimental data for their checking. The current information on the PCs efficiencies, beam profiles, angular $\theta_X, \theta_Y, \theta_Z$ (deflection angle at the analysing magnet), TOF and energy loss spectra, etc., was available.

The off-line treatment and analysis of the accumulated statistics under the condition $Tr1 = Gx * S1 * ST * \bar{A}$ were carried out in the following procedure:

1. For each energy and each kind of the target, the momentum spectra of the detected particles were obtained under a number of processing conditions to select the true elastic charge-exchange events. The momentum spectra were obtained under the following conditions:

- a) without any cuts;
- b) NOT DTS rejects inelasticities by the DTS signal which is the logic sum of all DTS scintillator signals;
- c) AND TOF selects events with the TOF response;
- d) using AND TOF together with a cut of the secondary deuteron admixture;
- e) application of logic AND for b) and d) criteria.

Then, taking into consideration the $M2$ monitor counts for the filled and empty targets, the momentum spectra (*filled* minus *empty*) were obtained under the above conditions.

2. The centers of the elastic charge-exchange peaks for the H_2 and D_2 targets (with subtracted E -contributions), were found using the corresponding momentum spectra obtained under condition e). The positions of the elastic peak centers for the D_2 target are shifted by about 6–8 MeV/ c towards the smaller values at all the beam energies with respect to the elastic peak centers for the H_2 target spectra. This is in agreement with the major part of existing results in the field (see, e.g., [14, 15]). The DTS efficiencies were determined while comparing the momentum spectra obtained under conditions e) and d). The values of the

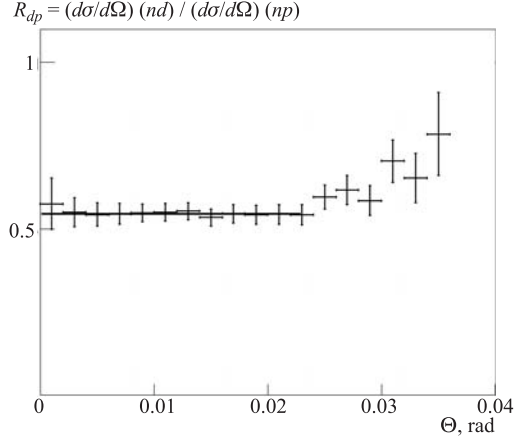


Fig. 8. The ratio R_{dp} angular distribution at $T_n = 1.0$ GeV

Table 6. Estimations of the systematical uncertainties at $T_n = 1.4$ GeV

Source of the systematics		Absolute values of the R_{dp} error
1.	Total PC efficiencies	0.0027
2.	Trigger PC efficiency	0.0026
3.	Efficiency of the DTS	0.0179
4.	Efficiency of the TOF -system	0.0034
5.	Error in shift determination of the H_2 and D_2 elastic peak center positions	0.0177
6.	Number of H/D nuclei in the targets	0.0014
Total:		0.0257

deuteron admixtures in the elastic peaks were calculated at each energy point from the comparison of the momentum spectra obtained under conditions d) and c).

3. The PC s and TOF efficiencies were calculated using the PC s coordinate information at each energy and for any kind of the target. The efficiency of each PC was calculated on the responses of the number of preceding and following (subsequent) PC s. The TOF efficiencies were found in the procedure of the particle track extrapolation into the TOF position area.

4. The angular distributions of the elastic event yields for H_2 and D_2 were obtained at the final stage of the data processing. For each θ_{Lab} bin of 2 mrad the H_2 and D_2 elastic yields were determined by the sum of the bin contents of the momentum distribution histogram over the range of 300–400 MeV/c from the maximum of the elastic peak. The angular distributions of the ratio $R_{dp}(\theta)$ were

determined taking into account the obtained PCs , DTS and TOF efficiencies as well as the $M2$ monitor counts and the n_H , n_D numbers of the target nuclei according to Eq. (1.4). An example of the ratio R_{dp} angular distribution at $T_n = 1.0$ GeV is shown in Fig. 8. Since the angular (by θ) dependence of the $R_{dp}(\theta)$ is almost constant within the spectrometer angular acceptance for all energy points, the final R_{dp} results were calculated as a weighted average of the R_{dp} values over the θ_{Lab} range from 0 to 16–30 mrad.

A detailed description of some set-up elements and the data treatment procedure will be done in separate publications.

The systematic errors of R_{dp} are mainly caused by the following: the uncertainties of the PCs , DTS and TOF efficiencies, the uncertainties of the n_H , n_D values and the uncertainties in defining the elastic peak center positions. The values of the systematic errors slightly vary for different energy values caused by the accumulated statistics and the temporary drifts of the PCs efficiencies. The sources and values of the systematic errors are listed in Table 6. Here the systematic errors are given at $T_n = 1.4$ GeV, as an example.

4. RESULTS

The R_{dp} results are presented in Table 7 and shown in Fig. 9. The total R_{dp} errors are the square root of the sums of the statistical and systematic uncertainties squared.

The obtained R_{dp} results are close to 0.56 and remain nearly constant with the energy over the investigated energy region. The earlier obtained R_{dp} results [17–31] (collected in [16]), are also plotted in Fig. 9. One of the first attempts of using the charge-exchange reaction on deuteron to extract the data on

Table 7. Values of $R_{dp} = d\sigma/d\Omega(nd \rightarrow pnn)/d\sigma/d\Omega(np \rightarrow pn)$ at $\theta_{p,Lab} = 0^\circ$. Total errors are the square root of the sums of the statistical and systematic uncertainties squared

NN	T_n , GeV	P_n , GeV/c	R_{dp}	Errors		
				Stat.	Syst.	Total
1	0.55	1.156	0.589	0.024	0.039	0.046
2	0.80	1.464	0.554	0.017	0.016	0.023
3	1.00	1.697	0.553	0.011	0.023	0.026
4	1.20	1.922	0.551	0.011	0.019	0.022
5	1.40	2.143	0.576	0.028	0.026	0.038
6	1.80	2.573	0.568	0.016	0.029	0.033
7	2.00	2.785	0.564	0.014	0.042	0.045

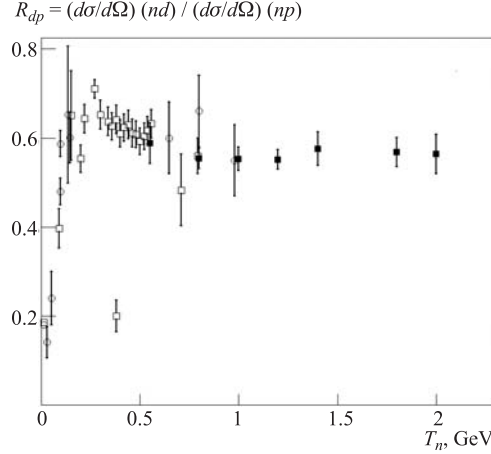


Fig. 9. The energy dependence for the R_{dp} results. Black squares — for this experiment, open squares and circles — for the existing data at lower energy from compilation [16]. The R_{dp} value at $T_n = 0.98$ GeV was taken from [33]

the spin-dependent part of the $np \rightarrow pn$ scattering amplitude was made [32] in the experiment with the hydrogen bubble chamber in the beam of deuterons at the momentum of 3.3 GeV/c. The R_{dp} value [33] at $T_n = 0.98$ GeV, obtained recently on the Dubna hydrogen bubble chamber data for $dp \rightarrow (pp)n$ reaction, is also shown in Fig. 9. All these data were measured below 1 GeV.

Our new R_{dp} results at the energy below 1 GeV are in a good agreement with the previous R_{dp} data. The main part of the present data is the first result obtained at the energy above 1 GeV.

5. CONCLUSIONS

These new results have been obtained for $R_{dp}(\theta_{p,\text{Lab}} = 0^\circ) = \frac{(d\sigma/d\Omega)(nd)}{(d\sigma/d\Omega)(np)}$ — the ratio of the quasi-elastic $nd \rightarrow p + (nn)$ charge-exchange yield to the free elastic $np \rightarrow pn$ yield at 0.55, 0.8, 1.0, 1.2, 1.4, 1.8 and 2.0 GeV.

These results at the energy below 1 GeV are in a good agreement with the previous R_{dp} data. The main part of the present data is the first result obtained at the energy above 1 GeV. We have observed that the R_{dp} values are relatively large (close to 0.56) and almost independent of energy, at least, up to 2 GeV.

The R_{dp} measurements at the energies above 2.0 GeV are planned to continue.

The used experimental method has provided accurate results. The systematic uncertainties are small since the ratio R_{dp} values were determined only by the measured relative values N_{targ} and M_{targ} while the reasonably quick replacement of the «full» and «empty» targets allowed us to avoid possible systematic errors caused by the influence of the temporary drifts of the detector efficiencies and other experimental conditions.

The comparison of the obtained data with the calculations of R_{dp} taken by using the invariant amplitude sets from the GW/VPI phase-shift analysis, was made in a separate paper [34].

Acknowledgements. The authors are grateful to the Synchrotron and Nuclotron staff, to all the scientific and engineering groups and individuals who took part and helped us in the measurements preparation, data taking and analysis. The personal support of C. Wilkin was favorable for our experiment. The authors thank the JINR, JINR VBLHE and DLNP Directorates for the support of these investigations. The work was in part financed by the Russian Foundation for Basic Research through Grant RFBR-07-02-01025.

REFERENCES

1. *Sharov V. I. et al.* // Proc. of the XVII Intern. Baldin Seminar on High Energy Physics Problems. Relativistic Nuclear Physics and Quantum Chromodynamics. Dubna, September 27 – October 2, 2004 / Eds. A. N. Sissakian, V. V. Burov, A. I. Malakhov. E1,2-2005-103, Dubna, 2005. P. 161.
2. *Sharov V. I. et al.* // Proc. of the Advanced Studies Institute on SYMMETRIES AND SPIN. (SPIN-PRAHA 2004). Czech Republic, Prague, July 5–10, 2004, Czech J. Phys. 2005. V. 55. P. A289.
3. *Sharov V. I. et al.* // Proc. of the XI Advanced Research Workshop on High Energy Spin Physics (DUBNA-SPIN-05), Dubna, Sept. 27 – Oct. 1, 2005 / Eds. A. V. Efremov, S. V. Goloskokov. E1,2-2006-105, Dubna, 2006. P. 424.
4. *Adiashevich B. P. et al.* // Zeitschrift für Physik C. 1996. Bd. 71. S. 65.
5. *Sharov V. I. et al.* // JINR Rapid Commun. 1996. No. 3[77]-96. P. 13.
6. *Sharov V. I. et al.* // JINR Rapid Commun. 1999. No. 4[96]-99. P. 17.
7. *Sharov V. I. et al.* // Eur. Phys. J. C. 2000. V. 13. P. 255.
8. *Sharov V. I. et al.* // Eur. Phys. J. C. 2004. V. 37. P. 79.
9. *Sharov V. I. et al.* // Yad. Fiz. 2005. V. 68, i. 11. P. 1858; Phys. At. Nuc. 2005. V. 68, i. 11. P. 1796.
10. *Derenchuk V. P. et al.* // 2001 Particle Acc. Conf. / Eds. P. Lucas, S. Webber, IEEE 01CH37268, 2003. 2001.
11. *Kirillov A. et al.* JINR Preprint E13-96-210. Dubna, 1996.

12. Ableev V. G. *et al.* // Nucl. Phys. A. 1983. V. 393. P. 941;
Nucl. Phys. A. 1983. V. 411. P. 514E.
13. Gorbunov N. V., Karev A. G. // Proc. of the XII Intern. Symp. on Nuclear Electronics, Varna, Bulgaria, Sept. 12–18, 1988, JINR D13-88-938. Dubna, 1989. P. 103.
14. Ball J. *et al.* // Eur. Phys. J. C. 1999. V. 11. P. 51.
15. de Lesquen A. *et al.* // Eur. Phys. J. C. 1999. V. 11. P. 69.
16. Lehar F. To be published in the review journal «Particles & Nuclei», JINR, Dubna.
17. Langsford A. *et al.* // Nucl. Phys. A. 1967. V. 99. P. 246.
18. Bonner B. E. *et al.* // Phys. Rev. C. 1978. V. 17. P. 664.
19. Pagels B. Diplomarbeit: Untersuchung der quasielastischen Ladungsaustauschreaktion $nd \rightarrow pnn$ im Neutronenergiebereich von 290 bis 570 MeV, Fakultät für Physik der Universität Freiburg im Breisgau. 1988 (unpublished).
20. Powell W. M. Preprint UCRL 1191. Berkeley, 1951.
21. Cladis J. R., Hadley J., Hess W. N. // Phys. Rev. 1952. V. 86. P. 110.
22. Hofmann J. A., Strauch K. // Phys. Rev. 1953. V. 90. P. 559.
23. Dzhelepov V. P. *et al.* // Izvestia Akad. Nauk. 1955. V. XIX. P. 573.
24. Larsen R. R. // Nuovo Cimento. 1960. V. XVIII. P. 1039.
25. Dzhelepov V. P. // Proc. of the Intern. Conf. on High Energy Physics, CERN, Geneva, 4–11 July 1962 / Ed. by J. Prentki. CERN, Geneva, 1962. P. 19.
26. Wong C. *et al.* // Phys. Rev. 1959. V. 116. P. 104.
27. Voitovetskii V. K., Korsunskii I. L., Pazhin Yu. F. // Nucl. Phys. 1965. V. 69. P. 531.
28. Batty C. J., Gilmore R. S., Stafford G. H. // Phys. Lett. 1965. V. 16. P. 137.
29. Esten M. J. *et al.* // Rev. Mod. Phys. 1965. V. 37. P. 533.
30. Measday D. F. // Phys. Lett. 1966. V. 21. P. 66.
31. Bjork C. W. *et al.* // Phys. Lett. 1976. V. 63B. P. 31.
32. Aladashvili B. S. *et al.* // Nucl. Phys. B. 1975. V. 86. P. 461.
33. Glagolev V. V. *et al.* // JINR Commun. P1-2006-112. Dubna, 2006.
34. Sharov V. I. *et al.* Submitted to «Yadernaya Fizika».

Received on April 30, 2008.

Редактор *В. В. Булатова*

Подписано в печать 20.08.2008.

Формат 60 × 90/16. Бумага офсетная. Печать офсетная.

Усл. печ. л. 1,31. Уч.-изд. л. 1,83. Тираж 425 экз. Заказ № 56278.

Издательский отдел Объединенного института ядерных исследований
141980, г. Дубна, Московская обл., ул. Жолио-Кюри, 6.

E-mail: publish@jinr.ru

www.jinr.ru/publish/